ELSEVIER

Journal of Chromatography A, 742 (1996) 211–227

JOURNAL OF CHROMATOGRAPHY A

Change of pH in electrophoretic zones as a cause of peak deformation

X. Xu, W.Th. Kok, H. Poppe*

Laboratory for Analytical Chemistry, University of Amsterdam, Nieuwe Achtergracht 166, 1018 WV Amsterdam, Netherlands

Received 13 November 1995; revised 3 March 1996; accepted 15 March 1996

Abstract

Electromigration dispersion (EMD) was studied theoretically with comparison of the results to experimental findings. The EMD behavior of a sample constituent in a given background electrolyte (BGE) could be described by an EMD constant, which determines uniquely the direction and the degree of a peak deformation into a triangular shape in a strong or a weak ion BGE system in capillary zone electrophoresis (CZE). The EMD constant was found to be proportional to the linear sum of the relative change of the electric field strength (conductivity effect) and the relative change of the effective mobility of the sample constituent (pH effect) across the steep boundary between sample and BGE zones. Based on the moving boundary model or equations, the two effects, as well as the EMD constants for different BGE types, can be calculated separately. Analytical solutions for those effects were also obtained for some simple cases. Computational results have shown that the conductivity effect and the pH effect for an analyte can be quite different with different BGE types. In some cases, the effects of conductivity and pH on EMD act in the same direction, and reinforce the peak broadening. In other cases they act in opposite directions, and therefore counteract each other partially or completely, leading to a relatively symmetric and narrower peak. To compare the contribution of each dispersion source, a variance of EMD, which is proportional to the EMD constant and time, was defined. It was found that the total variance of a peak can be approximated as the sum of the variance due to EMD and the variances due to other dispersion sources.

Keywords: Electromigration dispersion; Buffer composition; Moving boundary; Indirect detection; Dispersion; Overload columns; pH effects; Organic acids

1. Introduction

The background electrolyte (BGE) in capillary zone electrophoresis (CZE) serves as a medium to keep the electric field and the pH constant, in order to obtain constant effective mobilities of the sample constituents. Under ideal separation conditions and with low sample concentrations, molecular diffusion is the only source of zone broadening [1]. In that case, the only requirement on the BGE is to have adequate pH-buffering capacity at the pH required for the separation. However, a high sample-to-buffer concentration ratio is often required for reasons of detectability, especially using indirect detection, some techniques such as CE–MS, post-column reaction and in (micro)preparative applications. In such cases, one is often confronted with problems of concentration overloading. Overloading results in broader, triangular peaks and hence impairs the resolution. Concentration overloading, also known as

*Corresponding author.

0021-9673/96/$15.00
PII S0021-9673(96)00236-1

electromigration dispersion (EMD), is commonly explained as the result of the distortion of the electric field in the sample zone by the presence of the sample ions.

The phenomenon of EMD has been investigated over a long time; For instance, work was done by Hjerten [2] and Mikkers et al. [3,4]. They concluded that for a system with strong electrolytes the EMD can be eliminated by matching the mobility of the co-ion of the BGE to that of the sample ion. This result became known as the "ionic mobility match rule" or simply "μ-rule". When weak electrolytes and hydrogen or hydroxide ions are involved, the problem of EMD is much more difficult to solve. In 1989, Foret et al. [5] illustrated experimentally the role of EMD in a system containing mono- and poly-weak sample ions. They found that the sharpest peaks were those of components having an effective mobility close to that of the background electrolyte. This finding, known as the "effective mobility match rule" or simply "$\bar{\mu}$-rule", was later discussed theoretically by the same group [6].

Matching rules can be derived from Kohlrausch' regulating functions [7,8]:

$$\bar{\omega}_1 = \sum \frac{\bar{z}_i \bar{C}_i}{\mu_i} \tag{1}$$

$$\bar{\omega}_2 = \sum \bar{z}_i \bar{C}_i \tag{1b}$$

where $\bar{C}_i$ is the total concentration of the constituent i and $\bar{z}_i$ is $+1$ or -1, depending on the sign of the charged forms of constituent i. (Generally, in this paper, a bar over a symbol indicates that its value has to be summed or averaged over all ion species of a constituent). However, the Kohlrausch' functions are not sufficient to solve the problem of the EMD when the electrophoretic system contains a poly-weak electrolyte or more than one ionic constituent. Also, they can not be used for low- or high-pH BGEs, since in the second Kohlrausch' function it is assumed that the charge transport by hydrogen or hydroxide ions can be neglected. Therefore, the matching rules are only valid for a BGE containing a single strong electrolyte (μ-rule) or a single mono-weak electrolyte in the middle pH-range ($\bar{\mu}$-rule).

Recently, Wang and Hartwick [9] extended the μ-rule to a binary BGE system of strong ions. They showed that when a BGE was prepared from two visualization agents with different mobilities, good peak shapes could be obtained for analyte ions with a mobility close to that of either of these agents. However, they could not explain the disturbance peak (in fact, the system peak) with a mobility between those of the two BGE co-ion components.

The migration rate of a weak sample constituent in its zone can be dependent on its concentration as a result of a change in the conductivity, affecting the migration rate via changes in electric field, or as a result of a change in pH, affecting the migration rate by a change in the effective mobility of the compound. While the first mentioned effect has been studied extensively, the latter one has received much less attention. The effect of pH changes by overloading has only been mentioned briefly in several papers, for instance, [10–12]. A recent study [13], based on mass balances of co-ions and counter-ions of the BGE, described the influence of local pH changes on the effective mobility of sample constituents. However, it did not give an explicit description of the relationship between the conductivity and pH changes. Moreover, it neglected the migration of hydrogen and hydroxide ions.

A useful tool for studying EMD is the computer simulation program for CZE developed by our group [14]. The fundamentals of the numerical method of this program, in which various equilibria are considered and the basic laws of electrophoretic transport are applied, have been described before [15]. The program allows one to predict the migration rate of the sample constituent as a function of its concentration and consequently all effects of EMD, in all pH ranges, and to predict peak shapes and system peaks. The program can handle rather complicated electrophoretic systems, with sample and BGE components having up to five protolytic equilibrium steps, and up to four independent BGE constituents. The predictions of this numerical approach are in agreement with analytical expressions for those cases where the latter can be derived with simplifying approximations.

Electropherograms simulated by this program have shown that the μ-rule and the $\bar{\mu}$-rule are not universally applicable. For example, two symmetric peaks can be obtained with just a single BGE, and a symmetric peak can sometimes be obtained for a constituent having an ionic mobility and an effective mobility that are close neither to the ionic mobility

nor to the effective mobility of the co-ion of the BGE.

In the work presented in this paper, the two causes of EMD, conductivity and pH changes, and their mutual interaction have been studied. Theoretical results have been compared with computer simulations and with experimental electropherograms. General conditions and key parameters to obtain a minimum EMD will be discussed.

2. Theory

2.1. Electromigration dispersion (EMD) constant

Sample constituents with different mobilities in an injection plug start to split into separated sample zones when an electrical current is passed through the capillary. The velocity of an individual sample ion may vary with changes of the sample concentration along the migrating zone. The sample ion in a region with a higher concentration may move faster or slower than at a lower concentration, which results in a more or less triangular zone with a steep front on one side and a ramp on the other side, of course, with the actual shape modified by diffusion. The difference between the migration distances of the sample constituent on both sides of the zone increases with the migration time. This type of zone broadening, which is called electromigration dispersion (EMD), is illustrated in Fig. 1.

In Fig. 1, it is assumed that the velocity of a sample ion in the sample zone α close to the steep boundary ($\bar{\nu}_S^{\alpha}$) is higher than the velocity in the BGE zone β ($\bar{\nu}_S^{\beta}$). Also the steep front has a higher velocity in this case. After passing the current for a time increment Δt the sample zone width will be increased by $(\bar{\nu}_S^{\alpha} - \bar{\nu}_S^{\beta})\Delta t$.

In electrophoresis it has been generally found that to a good approximation the velocity of a sample constituent in its zone is linearly dependent on the ratio of its concentration and that of the BGE. Since the velocity (difference) is generally proportional to the field strength, the velocity of the steep front of the zone ($\bar{\nu}_S^{\alpha}$) can be expressed as:

$$\bar{\nu}_S^{\alpha} = \bar{\nu}_S^{\beta} + k_{EMD} E^{\beta} \frac{\bar{C}_S^{\alpha}}{C_{BGE}} \quad (2)$$

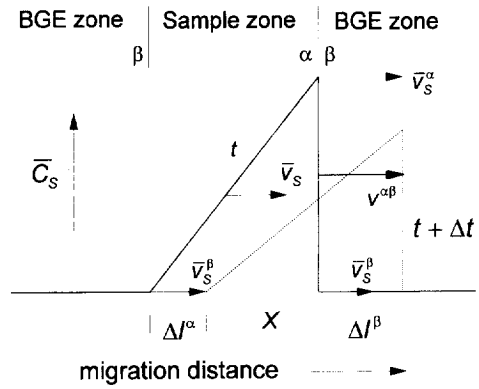

Fig. 1. Schematic representation of peak broadening due to electromigration dispersion (EMD) in CZE. The width of the sample zone increases from $\Delta l^{\alpha} + x$ to $\Delta l^{\beta} + x$ with a passage of an electric current for a short time Δt, because the velocity of the sample constituent ($\bar{\nu}_S$) changes with its own concentration ($\bar{C}_S$).

where the $\bar{C}_S^{\alpha}$ is the concentration of the sample constituent at the steep boundary and C_{BGE} is some convenient measure of the BGE concentration in the β solution, which will be discussed later. The EMD constant k_{EMD}, as defined by Eq. (2), describes the direction of the EMD and the sensitivity of a sample–BGE combination to overloading.

In our next paper we will give evidence for the accuracy generally obtained with this approximation. At this point we just note that the results obtained with the computer program described in Ref. [14] nearly always justify this procedure.

For a sample constituent in a given BGE, the EMD constant k_{EMD} remains unchanged during the CZE process and uniquely determines the EMD behavior of the sample constituent.

The concentration of the charged forms of a constituent in the BGE which dominates the EMD of the sample constituent is chosen as C_{BGE}. Usually it is equal to the concentration of the strong ion of the buffer mixture. With a multiple-ion BGE, an arbitrary dicision on the choice of the concentration C_{BGE} has to be made [9].

2.2. Conductivity and pH-shift effects

From the definition of a mobility $\bar{\mu} = \bar{\nu}/E$, we have:

$$\frac{\bar{\nu}_S^{\beta}}{E^{\beta}} = \bar{\mu}_S^{\beta} \text{ and } \frac{\bar{\nu}_S^{\alpha}}{E^{\beta}} = \frac{\bar{\mu}_S^{\alpha} E^{\alpha}}{E^{\beta}} \quad (3)$$

Combining Eqs. (2) and (3) gives:

$$k_{EMD} = \frac{\bar{\mu}_S^\beta}{\bar{C}_S^\alpha / C_{BGE}} \left(\frac{\Delta E}{E^\beta} + \frac{\Delta \bar{\mu}_S}{\bar{\mu}_S^\beta} + \frac{\Delta E \, \Delta \bar{\mu}_S}{E^\beta \bar{\mu}_S^\beta} \right)$$
$$\approx \frac{\bar{\mu}_S^\beta}{\bar{C}_S^\alpha / C_{BGE}} \left(\frac{\Delta E}{E^\beta} + \frac{\Delta \bar{\mu}_S}{\bar{\mu}_S^\beta} \right) \quad (4)$$

where $\Delta E = E^\alpha - E^\beta$ and $\Delta \bar{\mu}_S = \bar{\mu}_S^\alpha - \bar{\mu}_S^\beta$.

Furthermore, when the sample zone is not extremely broad, it holds that E^β is a constant equal to V/L, where V is the voltage applied to the tube and L is the tube length. Since the current density is uniform over the tube, we have:

$$J = E^\alpha \kappa^\alpha = E^\beta \kappa^\beta = \frac{V}{L} \kappa^\beta \quad (5)$$

where J is the current density and κ is the conductivity.

By reorganizing Eq. (5), the relative change of the electric field in Eq. (4) can be rearranged into:

$$\frac{\Delta E}{E^\beta} \cong \frac{-\Delta \kappa}{\kappa^\alpha} \quad (6)$$

where $\Delta \kappa = \kappa^\alpha - \kappa^\beta$.

By substituting Eq. (6) into Eq. (7), we have:

$$k_{EMD} = \frac{\bar{\mu}_S^\beta}{\bar{C}_S^\alpha / C_{BGE}} \left(\frac{-\Delta \kappa}{\kappa^\alpha} + \frac{\Delta \bar{\mu}_S}{\bar{\mu}_S^\beta} \right) \quad (7)$$

We assume that ionic strength effects on species mobilities and equilibrium constants are constant under CZE conditions. The changes in μ_S are then brought about exclusively by shifts in the acid–base equilibria, brought about by changes in pH. Therefore, Eqs. (4,7) show that the EMD in CZE consists of two effects: (1) the change of the electric field strength as a result of the conductivity change (κ effect) and (2) the change of the effective mobility as a result of the pH change (pH effect).

The effective mobility $\bar{\mu}$ of a constituent, the average of ionic mobilities of all of the subspecies, can be calculated in the way described by Tiselius [16], provided that the acid–base constants as well as the ionic mobilities of the various protonated forms of the constituent are known:

$$\bar{\mu}_i = \sum \alpha_j \mu_j \; (j = 0, \ldots, n) \quad (8)$$

where μ_j is the ionic mobility of subspecies j; $\bar{\mu}_i$ is the effective mobility of constituent i and α_j is the fraction of the subspecies j having j bound hydrogen ions of a constituent possessing n complexed hydrogen ions. The value of α_j at a given pH can be calculated by the well known equation:

$$\alpha_j = \frac{[H]^j K_0 K_1 \cdots K_j}{1 + [H]K_1 + [H]^2 K_1 K_2 + \cdots + [H]^n K_1 K_2 \cdots K_n}$$
$$(j = 0, \ldots, n) \quad (9)$$

where the K_j are the successive formation constants of the subspecies with j hydrogen ions and $K_0 = 1$.

As a special case, the relative change of the effective mobility for a monoweak ion is:

$$\frac{\Delta \bar{\mu}_S}{\bar{\mu}_S^\beta} = \frac{\Delta \alpha_S}{\alpha_S^\beta} \quad (10)$$

where $\Delta \alpha_S = \alpha_S^\alpha - \alpha_S^\beta$ and α_S is the fraction of the charged form of the monoweak ion.

2.3. General solution for the EMD constant — the moving boundary model

It is apparent from Eqs. (4) and (7) that solving the problem of EMD is equivalent to knowing the conductivities and pHs in both solutions α and β. The conductivity and pH in the β solution can be easily calculated from the known composition of the BGE. However, to find the values for the α solution it is first required to find the composition of the α solution. It is well known that two electrophoretic solutions separated by a moving boundary are related by Kohlrausch' regulating functions (Eq. 1) or moving boundary equations, the two basic foundations governing the electrophoresis [7]. In other words, the two solutions are regulating each other. Consequently, in principle, the composition of one solution can be obtained by the known composition of another solution. However, in practice the Kohlrausch' regulating functions are only useful for some very simple cases. The alternative, used here in the numerical work, is to employ the moving boundary equations to solve the problem of the EMD constant.

Consider the steep boundary of a single sample zone consisting of n constituents. The equations describing such a moving boundary for weak elec-

trolyte systems have been derived by Svensson [17] and Alberty [18] and may be written as:

$$\frac{\bar{\mu}_i^{\alpha}\bar{C}_i^{\alpha}}{\kappa^{\alpha}} - \frac{\bar{\mu}_i^{\beta}\bar{C}_i^{\beta}}{\kappa^{\beta}} = \frac{\nu^{\alpha\beta}}{J}(\bar{C}_i^{\alpha} - \bar{C}_i^{\beta}) \qquad (i = 1, \ldots, n) \tag{11}$$

This equation can be applied to any constituent i in the solutions α and β which are separated by a steep boundary produced by the passage of current. The quantity $\nu^{\alpha\beta}$ is the velocity of the steep boundary. The conductivities of the two solutions are κ^{α} and κ^{β}. The conductivity is given by the expression:

$$\kappa = F \cdot 1000 \sum_i \sum_j z_{ij}\mu_{ij}C_{ij}$$

(i for all constituents, j for all ions) (12)

where z_{ij}, μ_{ij} and C_{ij} denote the charge number, the ionic mobility and the concentration of j subspecies of all species in solution which comprise the i constituent, respectively.

Since the sample constituent is not present in the β solution, Eq. (11) for the sample constituent becomes:

$$\frac{\bar{\mu}_S^{\alpha}}{\kappa^{\alpha}} = \frac{\nu^{\alpha\beta}}{J} \tag{13}$$

Combining Eqs. (11) and (13), the general moving boundary equations for a weak ion system in CZE are obtained:

$$\bar{\mu}_i^{\alpha}\bar{C}_i^{\alpha} - \frac{\bar{\mu}_i^{\beta}\bar{C}_i^{\beta}\kappa^{\alpha}}{\kappa^{\beta}} = \bar{\mu}_S^{\alpha}(\bar{C}_i^{\alpha} - \bar{C}_i^{\beta}) \tag{14}$$

The equation set above may be applied to any constituent except for the sample constituent in the α and β solutions. However, a special "constituent" is formed by the protons, either present as "hydrogen ion", (e.g., H_3O^+), or bound to bases forming undissociated acids. The treatment of this proton constituent is mathematically tedious. One way to avoid this is to use Eq. (14) only for all the other constituents and to calculate pH (H_3O^+ and OH^-) afterwards as dependent variables from the equations of electroneutrality condition and the constant of the ionic product of water equilibrium [14]. Then the independent variables of $n-3$ concentrations (of all constituents except those of sample, proton and hydroxide) and the pH in the α solution can be found, from the $n-3$ moving boundary equations, the electroneutrality condition and the water autoprotonizing constant, under the following assumptions: (1) All quantities in the β solution and the sample constituent concentration in the α solution are known. (2)The ionic mobilities and the formation constants of constituent species are known and unchanged when they cross the steep boundary.

Eventually the relative change of the conductivity and the effective mobility across the steep boundary, or the EMD-constant, are calculated from the calculated constituent concentrations, and the pH in the α solution.

The complete equation set can be solved numerically with the help of a standard mathematics software package.

2.4. Analytical expressions for the EMD constant in monoweak ion systems

When the sample constituent is a strong or monoweak ion of the form HS/S^- or HS^+/S and the BGE also contains only one strong and one monoweak ion, accurate analytical expressions for the conductivity and the pH effect can be derived (see Appendix). These derivations are based on a linearization of the Kohlrausch' functions (Eq. 1), in which the charge transport by hydrogen and hydroxide ions is neglected. Therefore, the expressions will only be valid in the middle pH range. The expressions derived depend on the acid/base type of the BGE constituents, in relation to the type of sample ion. BGEs can be classified in this respect into four different types, as given in Table 1. The analytical expressions derived for types I to IV are given in Table 2.

Table 1
Classification of BGE

BGE type	Sample	BGE	
I	S^-	A^+	R^-
	S^+	A^-	R^+
II	HS^+/S	A^-	HR^+/R
	HS/S^-	A^+	HR/R^-
III	HS^+/S	HA/A^-	R^+
	HS/S^-	HA^+/A	R^-
IV	HS^+/S	HA/A^-	HR^+/R
	HS/S^-	HA^+/A	HR/R^-

* R = BGE co-ion; A = BGE counter-ion.

Table 2
Analytical expression for the conductivity effect and the pH effect for monoweak ion systems

BGE type[a]	C_{BGE}	Analytical solution for		Eqn.
		Conductivity effect[b]	pH effect[b]	
I	C_R	$\frac{\alpha_S(\mu_R-\mu_S)(\mu_A-\mu_S)}{(\mu_A-\mu_R)}$	0	15
II	C_A	$\frac{\alpha_S(\mu_R-\mu_S)(\mu_A-\bar{\mu}_S)}{(\mu_A-\mu_R)}$	$\frac{\bar{\mu}_S(1-\alpha_S)^2}{1-\alpha_R}+\frac{\alpha_S(1-\alpha_S)\mu_R(\mu_S-\mu_A)}{(\mu_A-\mu_R)}$	16
III	C_R	$\frac{\alpha_S(\mu_R-\bar{\mu}_S)(\mu_A-\mu_S)}{(\mu_A-\mu_R)}$	$\frac{\bar{\mu}_S(1-\alpha_S)^2}{1-\alpha_A}+\frac{\alpha_S(-1+\alpha_S)\mu_A(\mu_S-\mu_R)}{(\mu_A-\mu_R)}$	17
IV	C_R	$\frac{\alpha_S(1-\alpha_R)(\bar{\mu}_A-\bar{\mu}_S)(\bar{\mu}_R-\alpha_R\mu_S)+V(1-\alpha_A)(\bar{\mu}_R-\bar{\mu}_S)(\bar{\mu}_A-\alpha_A\mu_S)}{(\bar{\mu}_AV-\bar{\mu}_R)[\alpha_R(1-\alpha_R)+V\alpha_A(1-\alpha_A)]}$	$\frac{\alpha_S(1-\alpha_S)[\bar{\mu}_A(\mu_R-\mu_S)+\bar{\mu}_R(\mu_S-\mu_A)\bar{\mu}_S(\mu_A-\mu_R)]}{(\mu_R-\mu_A)[\alpha_R(1-\alpha_R)+V\alpha_A(1-\alpha_A)]}$	18

[a] See Table 1.

[b] Conductivity effect $=\bar{\mu}_S^{\beta}(\Delta E/E^{\beta})/(\bar{C}_S^{\alpha}/C_{BGE})$; pH effect $=\bar{\mu}_S^{\beta}(\Delta\bar{\mu}_S/\bar{\mu}_S^{\beta})/(\bar{C}_S^{\alpha}/C_{BGE})$. α_i is the ionization degree of the monoweak ion i; C_{BGE} is a convenient measure of the concentration of BGE (see text) and V is equal to C_A/C_R. All quantities in the table are those in the ß solution.

The expressions in Table 2 may be helpful for explaining some of the features of EMD observed experimentally. For instance, with a strong analyte ion in a strong BGE (type I), where there is no pH effect, Eq. 15 shows that the μ-rule applies, i.e., symmetric peaks will be observed when the mobility of the strong analyte ion matches that of the BGE co-ion. Eqs. (16) and (17) show that the μ-rule and the $\bar{\mu}$-rule may apply for BGE types II and III, respectively, when the sample constituent is strongly ionized at the pH-value of the BGE ($\alpha_S \rightarrow 1$). It is also shown that, in all cases, the pH- and the conductivity effects can be made smaller by choosing a BGE counter-ion with a large absolute mobility.

Table 2 shows that both effects can have a positive or a negative value. Therefore, conditions may be found where the two effects cancel each other, although finding such conditions is not straightforward. However, the equations given can be used to estimate the performance of a particulate BGE in terms of EMD. Moreover, when different buffer systems can be used, giving the pH appropriate for the separation of certain sample components, their EMD performances can be compared.

2.5. Relationship between the peak width and the EMD constant

In general, it may be assumed that the concentration of a sample constituent is changing linearly with the distance in a (triangular) sample zone. Since the sample constituent in the sample zone must match the injected amount, the integral mass balance with respect to the sample amount can be expressed as:

$$\bar{C}_{S,0} l_{inj} = \frac{1}{2} W_{EMD} \bar{C}_S^{\alpha} \tag{19}$$

where $\bar{C}$ is the sample's concentration at the injection; l_{inj} is the injection length of the sample zone and W_{EMD} is the zone width developed at time, t.

The zone broadening dW_{EMD} in time dt is (Fig. 1):

$$dW_{EMD} = |\bar{\nu}_S^{\alpha} - \bar{\nu}_S^{\beta}| \, dt \tag{20}$$

Combining Eqs. (2), (19) and Eq. (20), we have:

$$\int W_{EMD} \, dW_{EMD} = \frac{2E^{\beta} l_{inj} \bar{C}_{S,0} |k_{EMD}|}{C_{BGE}} \int dt \tag{21}$$

If this expression is integrated, the result is:

$$W_{EMD}^2 = \frac{4E^{\beta} l_{inj} \bar{C}_{S,0} |k_{EMD}| t}{C_{BGE}} \tag{22}$$

Here it is assumed that the sample injection length is much smaller than the width of the migration zone.

Eq. (22) shows that the peak width caused by EMD is proportional to the square root of the time, as is the case for regular dispersion. Therefore, it lies at hand to treat it in the same way, using a variance (σ_{EMD}^2), defined as the second centralized normalized moment. For a triangle, this is equal to W_{EMD}^2. Thus, it follows:

$$\sigma_{EMD}^2 = \frac{2E^{\beta} l_{inj} \bar{C}_{S,0} |k_{EMD}| t}{9C_{BGE}} \tag{23}$$

3. Experimental

3.1. Apparatus

CZE was carried out using a Prince system (Lauer, Emmen, Netherlands) equipped with a linear UV detector Model 200 (Linear Instruments, Fremont, CA, USA). 50 μm I.D. untreated fused-silica capillaries with a total length of 60.0 cm and an effective length of 45.1 cm were obtained from Polymicro Technologies (Phoenix, AZ, USA). Sample injection was performed by compressed air (80 mbar for 3 s), unless stated otherwise. The output of the detector was fed to a Hewlett-Packard HP3394A integrator. The pH of a BGE was adjusted using an appropriate concentration of sodium hydroxide solution. Samples were dissolved in the running BGE.

All computation was accomplished on a 486DX PC. The numerical procedures available for solving simultaneous equations were performed with the program Mathematica version 4.0 (Wolfram Research, Champaign, IL, USA) and the concentrations in BGE were used as the starting values for the procedures.

All data for the mobilities and pK_a values were

obtained from the sources in Refs. [19–22] unless stated otherwise.

3.2. Chemicals

Acetic acid, 1-hexanesulphonic acid, 1-heptanesulphonic acid and 1-pentanesulphonic acid were obtained from Janssen Chimica (Netherlands); D-glucuronic acid and propionic acid were from BDH (UK); 2-ethylcaproic acid and 4-aminobenzoic acid were from Fluka (Switzerland); valeric acid and dodecanesulphonic acid were from Aldrich (Netherlands) and 2-methacrylic acid was from Merck (Germany).

4. Results and discussion

4.1. Linearity of the EMD effect

As a criterion for comparing different BGEs for a given sample constituent with respect to EMD, an EMD constant k_{EMD} has been defined. The "constant" here means that the value of k_{EMD} remains unchanged when different electrophoretic conditions, such as applied voltage, capillary length and concentration ratios are used, as it is only a function of the chemical properties of the sample components, the BGE and the pH.

This property of k_{EMD} is illustrated in Fig. 2. Here, results of calculations using the moving boundary equations are shown, giving the rate of the peak width increase $\Delta\bar{\mu}_S$ as a function of $\bar{C}_S^{\alpha}/C_{BGE}$. The difference between the velocity of the sample constituent in the α solution and in the β solution keeps decreasing during electrophoresis, in proportion to the decrease in the concentration of the sample constituent in the α solution, because of the zone broadening. However, the ratio of the velocity difference to the concentration is almost constant, as is shown by the linear relationship between them. Thus, at least in these cases, k_{EMD} is approximately independent of the concentration ratio and migration time or length.

4.2. EMD of monoweak constituents

The condition for symmetric zones is that $k_{EMD}=0$. From Eq. (7) it follows that, apart from the case

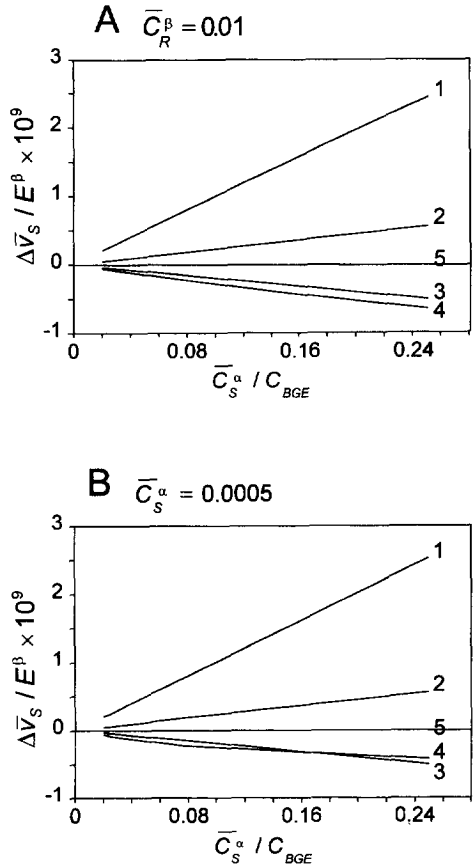

Fig. 2. The linear relationship between the velocity difference of a sample constituent in α and β solutions $\Delta\bar{v}_S$ and the concentration ratio of sample to BGE, with BGE type II for monobasic acids. Model BGE, 10 mmol/l of monobasic acid ($pK_{a,R}$ 4.9)+NaOH, pH 4.9. The conditions ($pK_{a,S}-pK_{a,R}$, μ_S/μ_R) for each line are, (1) −0.75, 1.3; (2) 0, 1.3; (3) 0, 0.7; (4) −0.75, 0.7; (5) 0, 0. $C_{BGE}=1/2\ \bar{C}_R^{\beta}$.

when the sample is neutral ($\bar{\mu}_S^{\beta}=0$) and co-migrates with the electroosmotic flow, this is realized when:

$$\frac{-\Delta\kappa}{\kappa^{\alpha}}+\frac{\Delta\bar{\mu}_S}{\bar{\mu}_S^{\beta}}=0 \qquad (24)$$

In other words, there are two conditions at which a symmetric zone can be achieved for a non-neutral sample. One is when both terms in the equation above are zero, i.e., the conductivity and pH effects are both zero. The second is when the two effects counteract each other.

For a strong ion system of BGE type I at any pH

only the conductivity effect exists, since there is no acid–base reaction across the steep boundary. Calculation of results shows that this effect is zero when the mobility ratio μ_S/μ_R equals one. This conclusion corresponds to the μ-match rule, which says that the EMD becomes larger with increasing differences between the mobilities of the sample ion and the co-ion.

For a weak ion BGE system of type II, the k_{EMD} values of a monoweak acid system, and the conductivity and pH effects contributing to them, are shown in Fig. 3A–C. The data shown were calculated for a sample-to-BGE co-ion concentration ratio of 1:20. The ratio of the ionic mobilities of the sample ion and the BGE co-ion was varied from 0.7 to 1.3 (lines 1–5); the ionization degree of the BGE co-ion was varied from 0.25 to 0.75 (columns A–C). The BGE is assumed to contain a monoweak acid as a co-ion with a pK_a of 4.9.

From Fig. 3A–C some general trends can be observed for the type II BGE.

(1) The conductivity effect is largely, but not solely, determined by the ratio of the ionic mobilities of the sample ion and the weak BGE constituent with the same charge. When the ionization degree of the BGE co-ion larger is than 50% ($\alpha_R > 0.5$), the μ-rule is valid for this effect, which is comparable with the analytical expression of Eq. 16.

(2) The conductivity effect is stronger when the ionization degree of the BGE is lower, i.e., when the BGE conductivity is lower.

(3) When the ionization degree of the BGE is low, the dependency of the conductivity effect on the pK_a value of the sample is stronger. This can be explained by the increased influence of hydrogen ion transport in the electrophoretic process.

(4) The pH-effect is small for sample components that are almost completely ionized in the BGE ($\alpha_S \rightarrow 1$).

(5) The pH-effect is small when the ionization degree of the sample is approximately equal to that of the BGE ($pK_{a,S} \approx pK_{a,R}$).

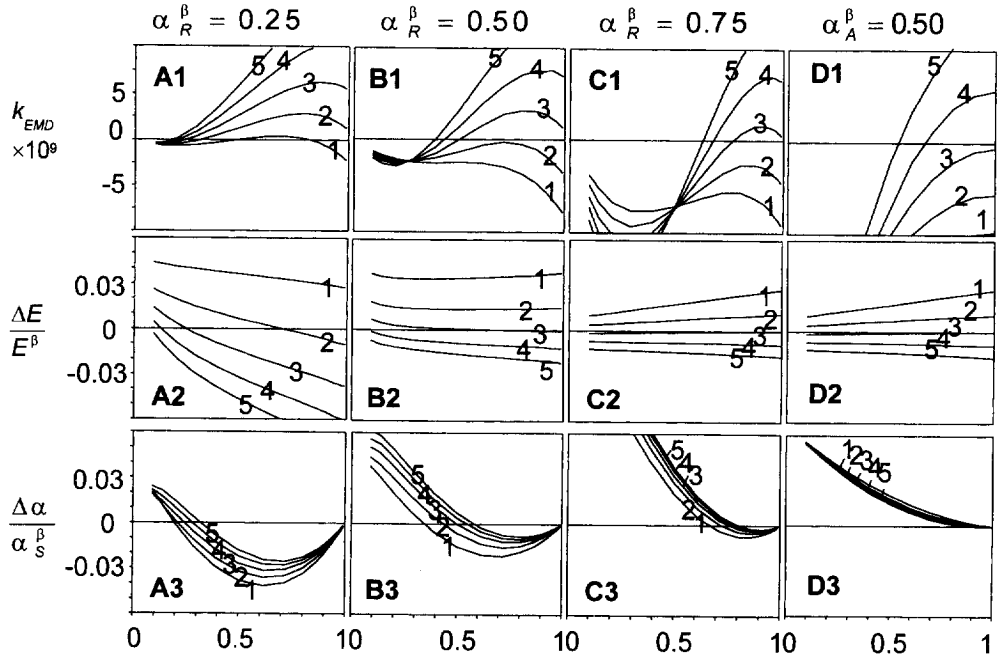

Fig. 3. Conductivity effect $\Delta E/E^{\beta}$, pH-effect $\Delta\alpha/\alpha^{\beta}$ and EMD constant k_{EMD}, in a monobasic acid system, as a function of (1) μ_S/μ_R in A–C or $\bar{\mu}_S^{\beta}/\bar{\mu}_R^{\beta}$ in D and (2) α_S^{β} the sample constituent ionization degree. (A–C), BGE type II with α_R^{β}, the BGE co-ion ionization degree, being (A) 0.75 (pH 5.4), (B) 0.5 (pH 4.9) and (C) 0.25 (pH 4.4). (D), BGE type III with BGE counter-ion ionization degree being 0.5 (pH 4.9). The ratios of (effective) mobilities for each line, (1) 0.6, (2) 0.8, (3) 1.0, (4) 1.2, (5) 1.4. Model BGEs, $pK_{a,R} = 4.9$ (A–C); $pK_{a,A} = 4.9$ (D). The ratio of the sample constituent to BGE co-ion concentration $\bar{C}_S^{\alpha}/\bar{C}_R^{\beta}$: 1/20; $\bar{C}_R^{\beta} \equiv 0.01$ mol l^{-1}.

(6) In some cases the pH and the conductivity effects reinforce each other, while in other cases they counteract and sometimes cancel each other, giving symmetric peaks ($k_{EMD}=0$).

Conditions leading to symmetric zones can be found from the points where the lines in Fig. 3 cross the zero$-k_{EMD}$ axis. In Table 3 the ionic and effective mobility ratios of the sample and BGE constituents are given for these points. It is shown that neither the μ-rule nor the $\bar{\mu}$-rule are generally valid. Occasionally one can find conditions where, for a number of sample constituents having similar ionic mobilities but different pK_a values (line 1 in Fig. 3A1) or different mobilities but similar pK_a values ($\alpha_S<0.3$ in Fig. 3B1), a low k_{EMD} value is obtained. For such a set of sample constituents all zones in an electropherogram would be relatively symmetric. However, it is difficult to formulate general rules for such conditions.

In column D in Fig. 3, the EMD characteristics are given for a type III BGE. The conditions are similar to those in Fig. 3B. However, the pH-buffering is obtained via the counter-ion and the ratio of effective mobilities are used for lines 1–5 instead of the ionic mobility ratio. In comparison to the data for a type II BGE with the same ionization degree (column B), the following differences are found:

(1) The conductivity effect is almost completely determined by the ratio of the effective mobilities of the sample ion and the strong BGE co-ion. The $\bar{\mu}$-rule is valid for this effect, which is comparable with the analytical expression of Eq. 17.

(2) The pH effect is almost independent of the effective mobility of the sample ion.

(3) The resulting value of k_{EMD} as a function of the effective mobility ratio is, in general, large.

Similar calculations have been performed for a BGE of type IV, containing two monoweak constituents with the same pK_a values as the pH. It was found that with such a buffer system neither the $\bar{\mu}$-rule nor the μ-rule is generally valid for the conductivity effect and the pH effect is smaller than with a type II or a type III BGE. Only when the sample ionization degree is less than 0.7, does the $\bar{\mu}$-rule applies.

Table 3
Cases for $k_{EMD}=0$ extracted from Fig. 5

	α_R^β	μ_S/μ_R	α_S^β	$\bar{\mu}_S^\beta/\bar{\mu}_R^\beta$
1)	0.75	1.0	0.75	1
2)	0.75	1.0	1.0	2
3)	0.75	1.2	0.68	1.1
4)	0.75	1.4	0.62	1.2
5)	0.5	0.8	0.72	1.14
6)	0.5	1.0	0.50	1
7)	0.5	1.0	1.0	2
8)	0.5	1.2	0.42	1.1
9)	0.5	1.4	0.38	1.1
10)	0.25	0.6	0.83	2.0
11)	0.25	0.6	0.48	1.1
12)	0.25	0.8	1.0	3.1
13)	0.25	0.8	0.31	1.0
14)	0.25	1.0	0.25	1.0
15)	0.25	1.2	0.21	1.0
16)	0.25	1.4	0.18	1.0

4.3. EMD of strong sample ions as a function of the pH

The calculations discussed in the previous paragraph have been performed for a monoweak buffering system with a pK_a of 4.9 and a pH in the range 4.4–5.4. However, we have found that the general rules obtained are valid for all such BGEs with a pH of between 4.5 and 9.5. However, for a BGE with a pH outside this range, the situation is more complex, due to the increased influence of the charge transport by hydrogen or hydroxide ions. Here, the relatively simple case of the EMD of strong ions in a type II BGE will be discussed.

EMD constants were again calculated by numerically solving the moving boundary equation set. Results obtained for strong anions in a HS/S$^-$ type II BGE are shown in Fig. 4. It is clear that, even when pH effects do not play a role, the behaviour of strong ions in a buffer with a high or low pH cannot be described by a simple matching rule. General trends observed from these and similar calculations are:

(1) For all pH values, the k_{EMD} of a strong ion depends on the mobility ratio of the sample and BGE constituents.

(2) In the pH range from 5 to 9, the μ-rule is valid for strong ions in a monoweak BGE.

(3) In low and high pH buffers, the k_{EMD} of a strong ion depends on the pK_a of the buffering constituent and the pH of the BGE.

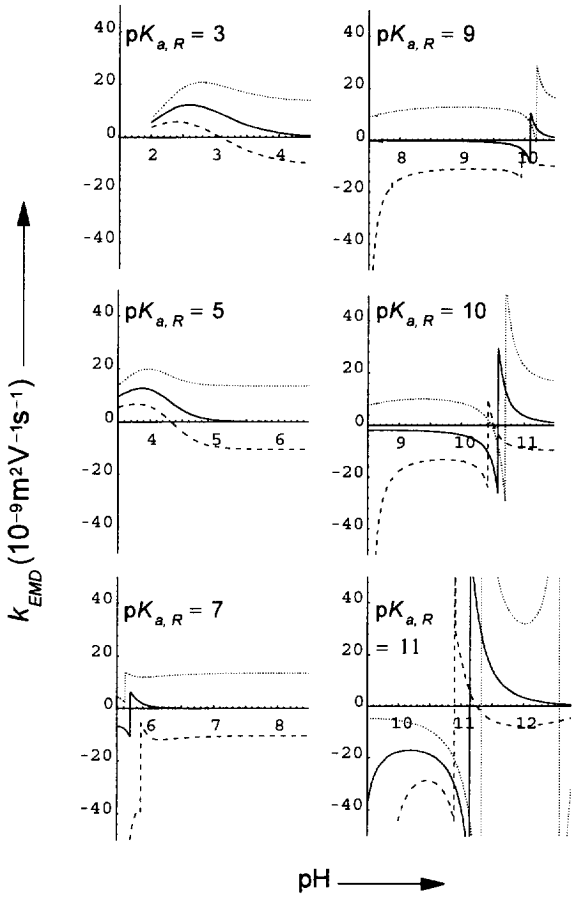

Fig. 4. EMD constant of a strong sample ion in BGE type II as a function of pH, with the ionic mobility ratio of the sample ion to BGE co-ion equal to 1.4 (dot line), 1.0 (solid line) and 0.6 (dash line) at a concentration ratio of $\bar{C}_S^{\alpha}/\bar{C}_R^{\beta}=1/20$.

(4) With a high pH BGE of type II, the shape of zones of strong anions may change from strongly tailing to strongly fronting by a small change of the BGE's pH. Similar behaviour was found for strong cations in a low pH buffer containing a weak cation as the co-ion.

4.4. Experimental evaluation

Fig. 5 shows the experimental separation of eight monoweak acids under the same conditions as described in Fig. 3B, with a BGE of 10 mmol l^{-1} of 4-aminobenzoic acid (4-ABA) ($pK_{a,R}=2.3$, 4.9, $\mu_R=-27.7$) and NaOH. The (zwitterionic) constituent 4-ABA had been selected as the BGE co-ion

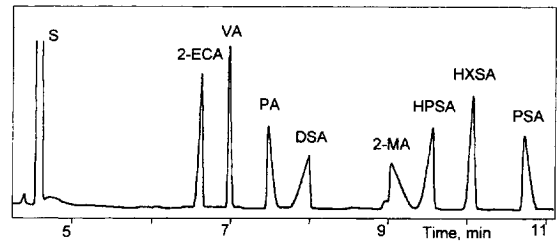

Fig. 5. Demonstration of the peak broadening due to conductivity and pH effects, by CZE separation of monobasic acids. Indirect UV detection, 267 nm; BGE, 10 mmol/l of 4-aminobenzoic acid + NaOH at pH 4.9; Temperature, 25°C. Separation, 300 V/cm; Pressure injection, 80 mbar/3 s; Sample concentration, 0.5 mmol/l each. Abbreviations, 2-ECA = 2-ethylcaproic acid; VA = valeric acid; PA = propionic acid; DSA = 1-dodecanesulphonic acid; 2-MA = 2-methacrylic acid; HPSA = 1-heptanesulphonic acid; HXSA = 1-hexanesulphonic acid; PSA = 1-pentanesulphonic acid. Numbers by peaks, values of $k_{EMD}\times 10^9$. Further details as in Table 4.

because it functions as a monobasic acid with a pK_a of 4.9 at the pH studied and meets the requirement to match the ionic mobilities of the sample ions of interest. The values of the two effects of conductivity and pH for each acid are listed in Table 4. It can be seen that the two symmetric peaks of valeric acid (VA) and 1-hexanesulphonic acid (1-HXSA) are in conditions leading to both $\Delta E\approx 0$ and $\Delta\alpha\approx 0$. The relative narrow peaks of 2-ethylcaproic acid (2-ECA) and propionic acid (PA) are in conditions in which the two effects (with different signs) are partially counteracting. The rather broad peak of 2-methacrylic acid (2-MA) is in a condition of the two effects acting in the same direction (the same sign). The acids 1-dodecanesulphonic acid (1-DSA), 1-heptanesulphonic acid (1-HPSA) and 1-pentanesulphonic acid (1-PSA) are strong ions at this pH, hence their EMD behavior is only dependent on the mobility ratio (pH effect is zero).

The ionic mobilities of all samples and of ABA itself were measured at pH 8.2.

It was found, as listed in Table 3, that the effective mobility ratio for a symmetric peak can be far from one. For instance, when the BGE parameters are set to let the pK_a value of BGE equal the pH ($\alpha_R^{\beta}=0.5$, $\bar{\mu}_R^{\beta}=0.5\mu_R$) and its ionic mobility is equal to that of the sample, it is possible that the sample peak becomes symmetric, with the effective mobility ratio being one or two. This is just the case for the peaks

Table 4
Data with respect to Fig. 5

	μ^a (10^{-9} m^2 V^{-1} s^{-1})	$\bar{\mu}^b$ (10^{-9} m^2 V^{-1} s^{-1})	pK_a	$\Delta E/E$	$\Delta\alpha/\alpha$	k_{EMD} (10^{-9} m^2 V^{-1} s^{-1})
Sample						
2-ECA	−23.73±0.08	−15.20±0.03	4.722	0.011	−0.0091	−0.29
VA	−28.20±0.08	−17.47±0.03	4.842	−0.001	0.0000	0.18
PA	−32.67±0.07	−20.17±0.05	4.874	−0.010	0.0050	1.01
DSA	−21.16±0.07	−20.90±0.01	<1	0.023	0	−4.80
2-MA	−33.22±0.09	−25.54±0.04	4.483	−0.015	−0.0088	6.08
HPSA	−26.00±0.06	−25.86±0.01	<1	0.0022	0	−0.57
HXSA	−27.48±0.11	−27.42±0.01	<1	−0.0010	0	0.27
PSA	−29.73±0.08	−29.21±0.01	<1	−0.0066	0	1.93
BGE						
4-ABA	−28.93±0.32	−13.82±0.01	2.38, 4.89			
Na^+	50.5					
EO[c]	52.09					

[a] Measured at pH 8.
[b] Measured at pH 4.9.
[c] Electroosmotic flow.

of VA and 1-HXSA in Fig. 5, where both the μ-rule and the $\bar{\mu}$-rule are valid for VA but only the μ-rule is valid for 1-HXSA.

Another possibility for getting a symmetric peak for a sample constituent of a weak ion is just to change the pH of the BGE to meet the second condition (the counteraction of the conductivity effect and the pH effect). Fig. 6 gives an example of this case. It is shown by the separations of acetic acid (p$K_{a,AA}$=4.75, μ=40.32) and glucuronic acid (pK_a=3.18, μ=24.99) in the BGE of 4-ABA (pK_a=4.90, μ=28.93). The peak of glucuronic acid changes its triangular peak direction from front tailing triangle to rear tailing triangle with the pH rising from 4.00 to 5.60, and becomes symmetric at pH 4.55. Under this condition, the effective mobilities of glucuronic acid and 4-ABA are 15.03 and 9.15, respectively, with the ionic mobility ratio being 0.86 and the effective mobility ratio being 2.54. This condition is close to the one in Table 3 (entry no. 10), which is predicted by the moving boundary model. Acetic acid does not become symmetric but becomes narrower when its effective mobility tends towards zero.

As can be seen from Table 3, symmetric zones only can be expected in the conditions of:

$$\alpha_S^\beta \le \alpha_R^\beta \ (pK_{a,S} \ge pK_{a,R}) \text{ and } \mu_S > \mu_R \quad (25)$$

$$\alpha_S^\beta \ge \alpha_R^\beta \ (pK_{a,S} \le pK_{a,R}) \text{ and } \mu_S < \mu_R \quad (26)$$

Because $pK_{a,Glu} < pK_{a,4\text{-}ABA}$ and $\mu_{Glu} < \mu_{4\text{-}ABA}$, according to Eqs. (25) and (26), it is possible to obtain a symmetric peak for glucuronic acid (Fig. 6) by changing the BGE's pH. However, acetic acid (Fig. 6) and 2-methacrylic acid (Fig. 5) do not meet

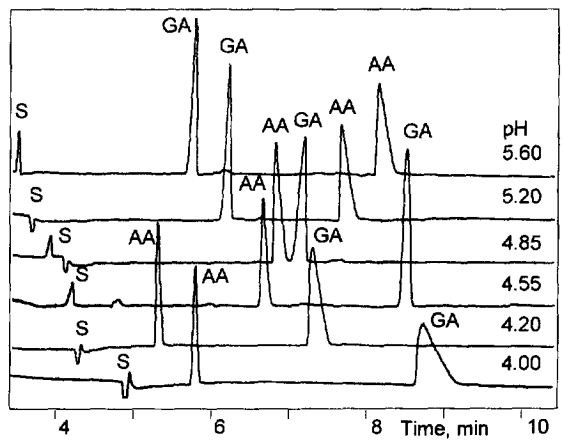

Fig. 6. The experimental evaluation of the pH effect on the EMD by using 10 mmol/l of 4-aminobenzoic acid as a buffer with the pH adjusted by appropriate strength NaOH and a mixture of acetic acid (AA) and glucuronic acid (GA) (0.5 mmol/l each) dissolved in the BGE as a sample. Indirect detection, 273 nm; temperature, 27.8°C. Other conditions, as described in Fig. 5.

the requirements in Eq. (25) or Eq. (26). When using a BGE composed of 4-ABA and NaOH, it is not possible to get these peaks symmetric just by changing the pH.

An example for BGE Type IV was shown experimentally, in [6], for the separation of four acids with a BGE composed of HIBA ($pK_{a,R}=4$) as a co-ion and aminobutyric acid ($pK_{a,A}=4$) as a counter-ion. Since the requirements, ($pK_{a,R}=pK_{a,A}=pH$ and $\alpha_S^\beta<0.7$), as described in Section 4.2 were met, the $\tilde{\mu}$-rule functioned there.

4.5. Relevance of the peak width with the EMD constant

In order to assess the separation efficiency for a deformed triangular peak, a theoretical plate number N, is introduced as [23]

$$N = l^2/\sigma_{tot}^2 \tag{27}$$

where l is the migration distance and σ_{tot} is the second moment of the peak in distance units in the zone taken about the mean and can be expressed as,

$$\sigma_{tot}^2 = W^2/18 \tag{28}$$

where W is the peak width at the baseline.

As known from a general formulation of the transport equation for CZE, the concentration distribution and, in turn, the second moment of the sample constituent in the migrating zone is developed in a complicated way, because of the EMD. From a practical point of view, there is a trend to look for a simple way to evaluate the contribution of each dispersion source. Foret et al. [24] assumed that the second moment can be the sum of the variances due to the particular sources of dispersion, including the EMD.

Following Foret, we assume:

$$\sigma_{tot}^2 = \sigma_{rest}^2 + \sigma_{Diff}^2 + \sigma_{EMD}^2 \tag{29}$$

where σ_{rest}^2 is the sum of the variances of injection, detection and temperature profiles due to the joule heat and so on, σ_{EMD}^2 is the partial second moment caused by the EMD and σ_{Diff}^2 is the variance of diffusion.

Under well-designed experimental conditions, σ_{rest}^2 can be very small and negligible. Thus σ_{tot}^2/t is proportional to the electric field applied, the injection length, the analyte concentration injected or the EMD constant, as seen in Eq. (22), if σ_{Diff}^2 is constant under the CZE condition. Their relationship is expressed schematically in Fig. 7. Fig. 8A–C has shown the plots of σ_{tot}^2/t versus E^β, l_{inj} and k_{EMD}/C_{EGE}, respectively. Different k_{EMD}/C_{EGE} values were obtained by using different BGE pHs, as seen in Fig. 6. The quite linear relationship between those variables implies that variances from different sources and that from EMD are approximately additive. Fig. 9 has illustrated the peak widths at different analyte concentrations injected. At pH 4.55, the EMD of glucuronic acid is nearly zero due to counteraction of the conductivity and pH effects. Its peak width remains approximately the same below a concentration of 2.5 mmol/l. Above this concentration, the moving boundary model is no longer valid.

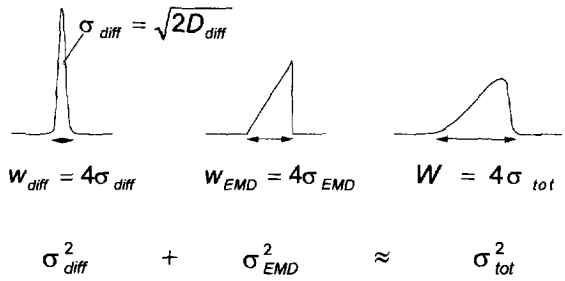

Fig. 7. Total peak broadening in CZE can be approximately expressed by the sum of the peak broadening caused by EMD and by other sources such as diffusion.

5. Conclusion

The migration rates of sample constituents in their zones turn out to be dependent on their concentrations as a result of changes in conductivity, affecting the migration rate via changes in electric field and (with protolyzing sample constituents), changes in pH, affecting the migration rate by changes in the effective mobility of the compound. This phenomenon can be described by the EMD constant defined in this paper, which is a criterion for the direction and degree of peak deformation in CZE. The problem of the two effects and their interaction has now been solved in three ways: (i) by solving means of the moving boundary equations

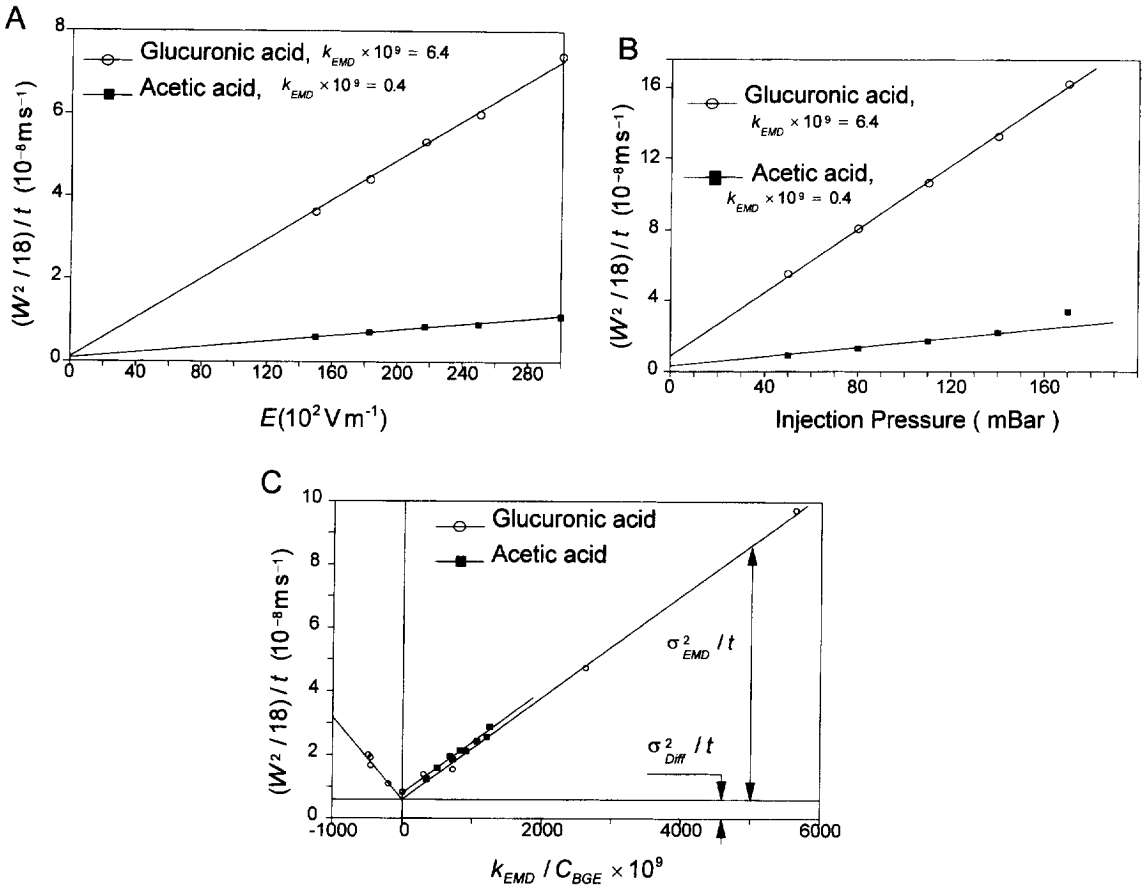

Fig. 8. Contribution of EMD to the peak broadening through (A) electric field applied, (B) injection (or injection pressure) and (C) EMD constant. Experimental conditions, pH 4.0 for (A) and (B), pH 4.0–5.6 for (C), the remainder are the same as in Fig. 6.

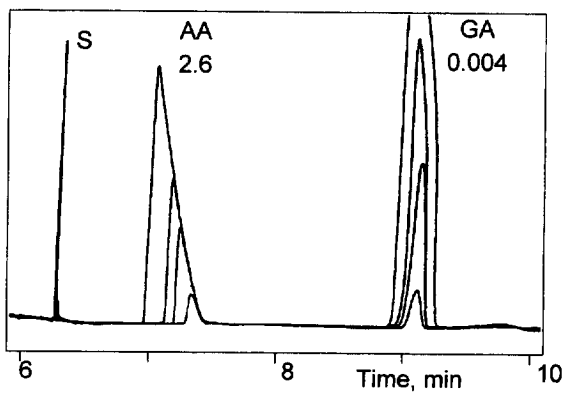

Fig. 9. Peak width change as a function of sample concentration. Concentration order (peak from top to bottom), 5, 2.5, 1, 0.25 mmol/l. Number by the peaks, values of $k_{EMD} \times 10^9$. pH 4.55. Other details as in Fig. 6.

numerically, (ii) by an analytical approximation described in the Appendix, and (iii) by means of an eigenvector description of the transport process [14]. The results of these methods are the same where this can be expected, which is the case for nearly all practical CE conditions. The total peak broadening is found to be approximately the sum of peak broadening caused by EMD and other sources.

Appendix 1

First order approximation of the dependence of migration rate on concentration as a result of conductivity and pH effects

In the following, the procedure will be explained for the case of a mono-basic neutral acid, HS, as a

solute, in a BGE consisting of a mixture of HR, a monobasic neutral acid, and A^+, a strong ion (case II, 2nd line, of Table 1). Equations for the cases II, 1st line and III 1st and 2nd line can be derived in an analogous fashion. The total concentration of each constituent has the indexed symbol c (c_S sample ion, c_R buffering ion, c_A strong ion), the fractions ionized are denoted by α_S and α_R. The two ω-relations are for this case:

$$-c_{R,\alpha}/\mu_R - c_{S,\alpha}/\mu_S + c_{A,\alpha}/\mu_A = -c_{R,\beta}/\mu_R - c_{S,\beta}/\mu_S + c_{A,\beta}/\mu_A \quad (\omega_1) \quad (A.1)$$

$$-c_{R,\alpha} - c_{S,\alpha} + c_{A,\alpha} = -c_{R,\beta} + c_{S,\beta} + c_{A,\beta} \quad (\omega_2) \quad (A.2)$$

In the usual case, the buffer does not contain S, so $c_{S,\beta}$ would be zero. In addition, we have a relation for the electroneutrality in the solute zone, α:

$$-\alpha_{R,\alpha}c_{R,\alpha} - \alpha_{S,\alpha}c_{S,\alpha} + c_{A,\alpha} = 0 \quad (En) \quad (A.3)$$

Moreover, we have a relation for the acid–base equilibrium in the α-zone:

$$\frac{\alpha_{R,a}(1-\alpha_{S,\alpha})}{(1-\alpha_{R,\alpha})\alpha_{S,\alpha}} = K_{rel} \quad (Eq) \quad (A.4)$$

where K_{rel} is the ratio of the dissociation constant of the buffer ion, $K_{a,R}$, to that, $K_{a,S}$, of the solute. This relation can be obtained by eliminating the hydrogen ion concentration between the two individual expressions for the dissociation constants. We will neglect the contribution of the hydrogen (and hydroxyl) ions to the conductivity, so it is indeed expedient to eliminate these quantities from the equations. The set of four equations allow us to find four variables that describe the α-zone, $c_{R,\alpha}$, $\alpha_{R,\alpha}$, $\alpha_{S,\alpha}$, and $c_{A,\alpha}$, as a function of the sample concentration, $c_{S,\alpha}$. With that, the effective mobility of the solute S, $\bar{\mu}_S$, and the local conductivity and the mean velocity of the solute can be found.

In the first step to arrive at an explicit expression, all quantities, which are functions of $c_{S,\alpha}$, are approximated as two-term Taylor series around the composition of the β-zone ($c_{S,\alpha}=c_{S,\beta}=0$):

$$c_{R,A} = c_{R,\beta} + c'_R c_{S,\alpha}$$

$$\alpha_{R,\alpha} = \alpha_{R,\beta} + \alpha'_R c_{S,\alpha}$$

$$c_{A,\alpha} = c_{A,\beta} + c'_A c_{S,\alpha}$$

$$\alpha_{S,\alpha} = \alpha_{S,\beta} + \alpha'_S c_{S,\alpha} \quad (A.5)$$

where the prime indicates the derivative with respect to $c_{S,\alpha}$. These approximations are substituted into the four equations, the result is differentiated with respect to $c_{S,\alpha}$ once, and the limit for $c_{S,\alpha}\to 0$ is taken. The resulting four equations are:

$$\frac{c'_A}{\mu_A} - \frac{c'_R}{\mu_R} - \frac{1}{\mu_S} = 0 \quad (A.6)$$

$$-1 + c'_A - c'_R = 0 \quad (A.7)$$

$$-\alpha_{S,\beta} + c'_A - \alpha'_R c_{R,\beta} - \alpha_{R,\beta}c'_R = 0 \quad (A.8)$$

$$\frac{(\alpha'_R\alpha_{S,\beta} - \alpha'_R\alpha^2_{S,\beta} - \alpha_{R,\beta}\alpha'_S + \alpha^2_{R,\beta}\alpha'_S)}{(-1+\alpha_{R,\beta})^2\alpha^2_{S,\beta}} = 0 \quad (A.9)$$

A solution of these four equations in the derivatives c'_R, α'_R, c'_A and α'_S is found as:

$$c'_R = \frac{\mu_R(-\mu_A+\mu_S)}{(\mu_A-\mu_R)\mu_S} \quad (A.10)$$

$$\alpha'_R = \frac{(-\alpha_{R,\beta}+\alpha_{S,\beta})(\mu_A-\mu_R)\mu_S + (-1+\alpha_{R,\beta})\mu_A(-\mu_R+\mu_S)}{c_{R,\beta}(\mu_A-\mu_R)\mu_S} \quad (A.11)$$

$$c'_A = \frac{\mu_A(-\mu_R+\mu_S)}{(\mu_A-\mu_R)\mu_S} \quad (A.12)$$

$$\alpha_S = \frac{(1-\alpha_{S,\beta})\alpha_{S,\beta}((-\alpha_{R,\beta}+\alpha_{S,\beta})(\mu_A-\mu_R)\mu_S + (-1+\alpha_{R,\beta})\mu_A(-\mu_R+\mu_S))}{(-1+\alpha_{R,\beta})\alpha_{R,\beta}c_{R,\beta}(\mu_A-\mu_R)\mu_S} \quad (A.13)$$

We note in passing that c'_R and c'_A are the replacement ratios as are relevant in indirect detection. They appear not to be dependent on the ionization degrees. The mean species velocity of S, normalized on the field in the β-zone (not strictly a mobility), $u_{S,\alpha}$, is found from:

$$u_{S,\alpha} = \alpha_{S,\alpha}\mu_S\frac{\kappa_\beta}{\kappa_\alpha} \quad (A.14)$$

The conductivities, κ_α and κ_β can be described as:

$$\kappa_\alpha = -\alpha_{R,\alpha}c_{R,\alpha}\mu_R - \alpha_{S,\alpha}c_{S,\alpha}\mu_S + c_{A,\alpha}\mu_A \quad (A.15)$$

$$\kappa_\beta = -\alpha_{R,\beta} c_{R,\beta} \mu_R + c_{A,\beta} \mu_A \quad (A.16)$$

Therefore, using A.5 and A6–A13, $u_{S,\alpha}$ and both values for κ can be expressed as a function of the solute concentration $c_{S,\alpha}$. Since the derivation is valid only provided $c_{S,\alpha}$ is small compared to the buffer concentrations, only two terms of a Taylor expansion for $u_{S,\alpha}$ are relevant:

$$u_{S,\alpha} = \alpha_{S,\beta} \mu_S + \frac{du_{S,\alpha}}{dc_{S,\alpha}} c_{S,\alpha} \quad (A.17)$$

The first term, $\alpha_{S,\beta}\mu_S$, or $\bar{\mu}_S$, is the velocity of S at infinite dilution. The second term follows from the differentiation of the full $u_{S,\alpha}$ expression, (A.14), with respect to $c_{S,\alpha}$. The result has to be multiplied by c_A, since k_{EMD} as defined in the main text was normalized on this "buffer concentration":

$$k_{EMD} = \frac{du_{S,\alpha}}{dc_{S,\alpha}} c_{BGE}, \quad (A.18)$$

where c_A has been chosen as the "convenient measure" for the buffer concentration, c_{BGE}. With this one finds after extensive manipulation:

$$k_{EMD}/\bar{\mu}_S = \frac{(\mu_R - \mu_S)(\mu_A - \alpha_{S,\beta}\mu_S)}{(\mu_A - \mu_R)\mu_S} + \frac{(1-\alpha_{S,\beta})^2}{1-\alpha_{R,\beta}} + \frac{(1-\alpha_{S,\beta})\mu_R(-\mu_A + \mu_S)}{(\mu_A - \mu_R)\mu_S} \quad (A.19)$$

as is given in Table 2. Note that the value of the equilibrium constant K_{rel} is "hidden" in the values of $\alpha_{S,\beta}$ and $\alpha_{R,\beta}$.

Use of equations from Table 2; species versus concentration velocity

Equations such as those in Table 2 and A.19 give the species velocity as a function of concentration. These can be used to directly calculate the migration rate $v_{\alpha\beta}$ ($=u_{S,\alpha}$) for a sharp front between a concentration of zero and a given concentration. However, in zone electrophoresis, the zone usually does not have a constant (maximum) concentration (triangular peaks, decreasing in height), and this way to predict the zone shape on elution is therefore tedious. It would require the integration of the travelled distance of the maximum over time, taking into account the decreasing concentration. When the injection block is not infinitely narrow, further complications would arise. It is therefore easier to first calculate the diffuse boundary of the zone. This is done by considering the "velocity of a concentration", $u_{S,c}$ (in the following equations, the index α has been omitted). Using the transport equation:

$$\frac{\partial c_S}{\partial t} = -\frac{\partial J_S}{\partial z}$$

where J_S is the flux of S, equal to $c_S \cdot u_S$, one finds for a point of constant concentration:

$$u_{S,c} = \left(\frac{\partial z}{\partial t}\right)_{c_S} = -\frac{\partial c_S/\partial t}{\partial c_S/\partial z} = \frac{\partial(c_S u_S)/\partial z}{\partial c_S/\partial z} = u_S + du_S/dc_S c_S \quad (A.20)$$

Inserting an equation such as A.19 for u_S as a function of c_S, the slope factor occurs twice in the result. The values of k_{EMD} thus have to be multiplied by two for the calculation of the diffuse boundary.

Once this is done, the velocity is known as a function of concentration. Also, the position (relative to the corresponding edge of the injection block) after a time t can be found for each concentration c_S in the diffuse boundary as the product $t\, u_{S,c}(c_S)$. The position of the maximum (and the sharp boundary) is next found by applying an integral mass balance; the area of the triangle must be equal to that of the original injection plug, i.e., to the amount injected. In rare (at least in CZE) cases the predicted maximum height is larger than the original injection concentration. If so, the maximum is flat, the original injection plug is still partially visible and a corresponding re-calculation has to be carried out.

References

[1] J.W. Jorgenson and K.D.A. Lukacs, Science, 222 (1983) 266–273.
[2] S. Hjerten, in G. Milazzo (Editor), Topics in Bioelectrochemistry and Bioenergetics, Vol. 2, Wiley, New York, p. 106.
[3] F.E.P. Mikkers, F.M. Everaerts and Th.P.E.M. Verheggen, J. Chromatogr., 169 (1979) 1.

[4] F.E.P. Mikkers, F.M. Everaerts and Th.P.E.M. Verheggen, J. Chromatogr., 169 (1979) 11.
[5] F. Foret, S. Fanali, L. Ossicini and P. Bocek, J. Chromatogr., 470 (1989) 299.
[6] V. Sustacek, F. Foret and P. Bocek, J. Chromatogr., 545 (1991) 239.
[7] F. Kohlrausch, Ann. Phys. Chem., 62 (1897) 209.
[8] L.M. Hjelmeland and A. Chrambach, Electrophoresis, 3 (1982) 9.
[9] T. Wang and R.A. Hartwick, J. Chromatogr., 589 (1992) 307.
[10] S. Hjerten, Electrophoresis, 11 (1990) 665.
[11] S.V. Ermakov, O.S. Mazhorova and M.Y. Zhukov, Electrophoresis, 13 (1992) 838.
[12] S.V. Ermakov and P.G. Righetti, J. Chromatogr. A, 667 (1994) 257.
[13] J.L. Beckers, J. Chromatogr. A, 693 (1995) 347.
[14] H. Poppe, Anal. Chem., 64 (1992) 1908.
[15] H. Poppe, J. Chromatogr., 506 (1990) 45.
[16] A. Tiselius, Nova Acta Regiae Soc. Sci. Upsaliensis [4] 7, No. 4, 1930, pp. 1–107.
[17] H. Svensson, Acta Chem. Scand., 2 (1948) 841.
[18] R.A. Alberty, J. Am. Chem. Soc., 72 (1950) 2361.
[19] T. Hirokawa, M. Nishino, N. Aoki, Y. Sawamoto, T. Yagi and J. Akiyama, J. Chromatogr., 271 (1983) D1.
[20] T. Hirokawa and Y. Kiso, J. Chromatogr., 628 (1993) 283.
[21] G. Kortüm, W. Vogel and K. Andrussow, Dissociation Constants of Organic Acids in Aqueous Solution, Butterworths, London, 1961.
[22] D.D. Perrin, Dissociation Constants of Organic Bases in Aqueous Solution, Butterworths, London, 1965.
[23] J.H. Knox and H.M. Pyper, J. Chromatogr., 363 (1986) 1.
[24] F. Foret, M. Deml and P. Bocek, J. Chromatogr., 452 (1988) 601.